

# Optical characterization of a semisolid membrane by high speed interferometry

DAVID ASAEL GUTIÉRREZ HERNÁNDEZ<sup>a\*</sup>, CARLOS PÉREZ LÓPEZ<sup>a</sup>, FERNANDO MENDOZA SANTOYO<sup>a</sup>, ALEJANDRO TÉLLEZ-QUIÑONES<sup>a</sup>, DANIEL D. AGUAYO<sup>b</sup>

<sup>a</sup>Centro de Investigaciones en Óptica, Lomas del Bosque 115. Col. Lomas del Campestre, C.P. 31715. León, Guanajuato, México

<sup>b</sup>Laboratory of biomedical Physics, University of Antwerp, Groenenborgerlaan 171, B 2020, Antwerpen, Belgium

In this paper, we present a high speed electronic speckle pattern interferometer (HSESPI) for the experimental analysis of a semisolid and rectangular membrane fully supported on its 4 edges. This system is based on an out of plane interferometer setup that integrates a continuous wave and a fast camera with an acquisition rate of 5000 frames/s. The acquired data is a set of temporal and full-field spatial samples of the surface deformation that have an optical phase change due to free vibrations coming from an external and random vibration frequency. Several fringe patterns of interference are contended all over the 5000 recorded frames. Each fringe pattern is processed by a phase extraction of a single fringe pattern algorithm. With this information, it is possible to do a spatiotemporal characterization of the membrane. The results shown graphics of a couple of points of the membrane followed along the time and the spatial evolution of a couple of profiles inside the membrane.

(Received April 22, 2014; accepted May 15, 2014)

**Keywords:** High Speed ESPI, Membranes, Transient vibrations

## 1. Introduction

ESPI is an optical technique that was first proposed (and almost simultaneously) in the early 70's by Butters and Leendertz [1], Makovski et al [2] and Schwomma [3] and has been widely applied to full-field measurements since then. There has been a particular interest on applying ESPI for industrial issues like dynamic measurements (flowing conditions, vibration and convection) and static measurements (displacement, torsion, refractive index and pressure) [4, 5, 6, 7, 8].

For this work, the ESPI system used to measuring vibrations over a semisolid membrane comprises two parts, the optical and the electronic part, as it is shown in Fig. 1.

In the optical part, the light source is a CW laser, which is separated into two coherent waves, the object,  $I_o$ , and the reference,  $I_r$ , by means of the beam splitter, BS1. The speckle patterns produced by both waves pass the beam combiner, BS2, to get an interference patterns on the sensor of the camera, which is a high speed CMOS camera for this work. The instantaneous value of the speckle pattern intensity at every image point of the object is encoded in the resulting interferogram, which is recorded by the camera and processed by a computer program in the electronic part of the system in order to reveals the information encoded in the interferograms.

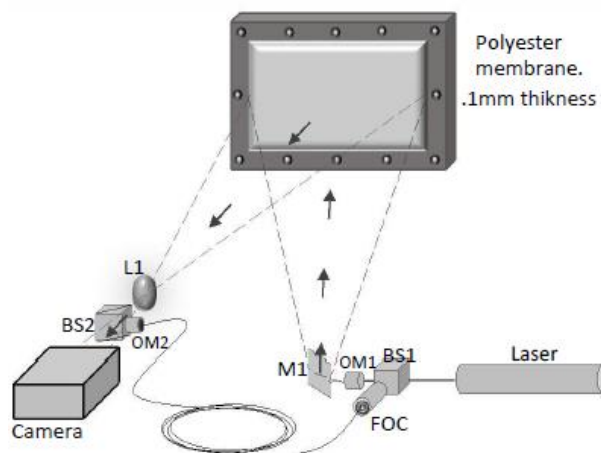


Fig. 1. Optical set-up for an out-of-plane sensitive ESPI. A continuous beam coming from a laser source with 6-Watts maximum and 532 nm wavelength, is divided by the beam splitter, BS1, into an object and a reference beams. OM1 is a 10x microscope objective that projects the object beam over the target. MO2 is a 10x microscope objective that projects the reference beam over the camera sensor trough a beam splitter, BS2, which also recombines the reflected intensity coming from the object into the camera. For this work, the laser is set to a power of 5.5 Watts and the CMOS camera is set to an exposure time of 5000 frames per second leaving the shutter permanently open.

The coherent addition of the two speckle fields coming from the reference and object beams will result in a third speckle pattern  $I(x, y)$  formed in the image plane of the sensor. The intensity distribution of this pattern is expressed as:

$$I(x, y) = I_o(x, y) + I_r(x, y) + 2\sqrt{I_o(x, y)I_r(x, y)}\cos[\psi(x, y)] \quad (1)$$

Where  $I_o(x, y)$  and  $I_r(x, y)$  are the speckle pattern intensity distributions coming from the object and the reference.  $\psi(x, y)$  is the phase difference between the reference and object speckles and is written as

$$\psi(x, y) = \phi_o(x, y) - \phi_r(x, y) \quad (2)$$

When a deformation happens, it changes the phase  $\phi(x, y)$  of each point by  $\Delta\phi(x, y)$ . In this case, equation (1) can be rewritten as

$$I'(x, y) = I_o(x, y) + I_r(x, y) + 2\sqrt{I_o(x, y)I_r(x, y)}\cos[\psi(x, y) + \Delta\phi(x, y)] \quad (3)$$

When (3) is subtracted from (1), the result gets the form

$$I(x, y) - I'(x, y) = 4\sqrt{I_o(x, y)I_r(x, y)}\sin\left[\psi(x, y) + \frac{\Delta\phi(x, y)}{2}\right]\sin\left[\frac{\Delta\phi(x, y)}{2}\right] \quad (4)$$

Where the square root describes the background illumination, the first sine factor gives the speckle noise, which is modulated by the second sine factor. This low frequency modulation of the high frequency speckle noise is very well known as fringe pattern of interference.

The principal function of the ESPI technique is to generate fringe patterns that can be processed by a variety of computational algorithms with the idea of extracting the phase representing the behavior of the object under study. Fig. 2 shows an example of a fringe pattern of interference coming from an ESPI system according to equation (4). In [9, 10, 11] are very well explained the basic principles of ESPI.

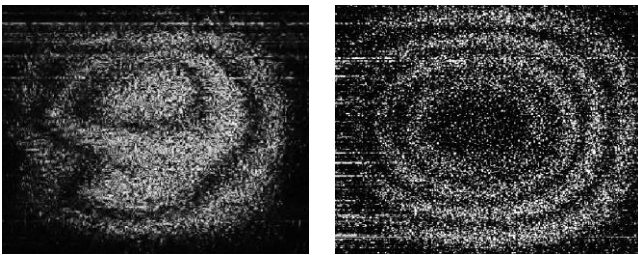


Fig. 2. Examples of fringe patterns of interference produced by the subtraction of two speckle interferograms with a change of phase between them.

## 2. Phase extraction of a single fringe pattern

Phase demodulation from a single fringe pattern offers to ESPI a big opportunity to venture in industrial applications under difficult conditions, for example, for transient vibrations measurements where it is not possible to repeat and synchronize the dynamic event with the electronic components of the ESPI. In recent years, some algorithms for phase extraction of single fringes have been published, some examples are shown in [12-18].

For this work, a function called DemIQT for the demodulation of fringe patterns with closed or opened fringes was used. This function belongs to a software called XtremeFringe, which was developed to be compatible with matlab instructions [19].

The function is based in the Isotropic Quadrature Transform, which is widely described in [20, 21]. Given the normalized version of a fringe pattern, the corresponding quadrature term can be get as

$$Q\{I_N\} = -\sin\phi \quad (5)$$

Where  $Q\{\}$  is the isotropic quadrature operator. The wrapped phase of the modulation phase can be obtained from

$$W\{\phi\} = \arctan\left(-\frac{Q\{I_N\}}{I_N}\right) \quad (6)$$

The demodulated phase obtained for the fringe pattern will give very useful information in order to analysis the behavior of the object under study.

For example, consider a simulated fringe pattern of interference as it is shown in Fig. 3a. Once it is processed by the proposed technique, the recovery phase is shown in Fig. 3b.

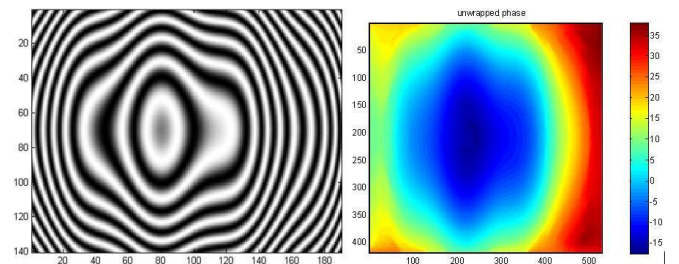


Fig. 3. Example of the phase recovery from a single fringe pattern. a) Simulated fringe pattern of interference, b) Phase recovered by means of the proposed technique.

From Fig. 3b, x-axis and y-axis are in pixels, but each pixel has a particular value of the phase recovered. With this information, it is possible to graphic the profile of the deformation over the object under study. Another example is suited in Fig. 4, where a simulated fringe pattern, with a parabolic phase of deformation was induced, is processed by the proposed technique. A couple of profiles from the

recovered phase are plotted, one on the x-axis and another one on the y-axis. Both profiles meet the parabolic form of

the phase used to simulate the fringe pattern.

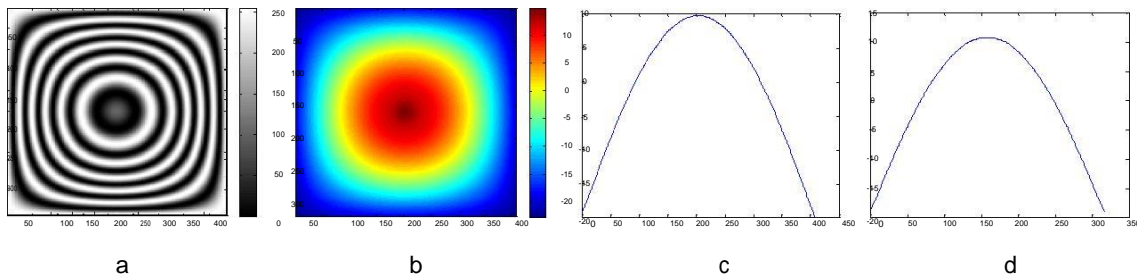


Fig. 4. a) Simulated fringe pattern with a parabolic phase, b) phase recovered by the proposed technique, c) profile of the phase values along the x-axis, d) profile of the phase values along the y-axis.

For Fig. 4a and 4b, x-axis and y-axis are in pixels, for Fig. 4c and 4d, x-axis is in pixels (but it can be expressed in meters) and y-axis is the phase value en radians.

### 3. Experimental results

A semisolid polyester membrane, under free vibrations, is studied by means of an ESPI system modified with a high speed CMOS sensor configured at 5000 fps and a continuous wave laser working on a wavelength of 532 nm and with a power of 3 Watts.

The first 1000 interference patterns recorded are considered for this experiment. Each of these patterns has a phase difference with respect to the others and depends

directly on the time changing. So thereby, it can be considered any of the interference patterns, at any time, as the initial state of the deformation of the membrane, taking the form of equation (1) and from then, the rest of pattern will take the form expressed on equation (3) where the phase,  $\Delta\phi(x, y)$ , changes directly to the membrane vibration. By subtracting all the interference patterns from the first selected as the initial state of deformation, there are hundreds of fringe patterns generated, all of them taking the form presented in equation (4). Fig. 5 shows only a few of the fringe patterns obtained from this experiment.

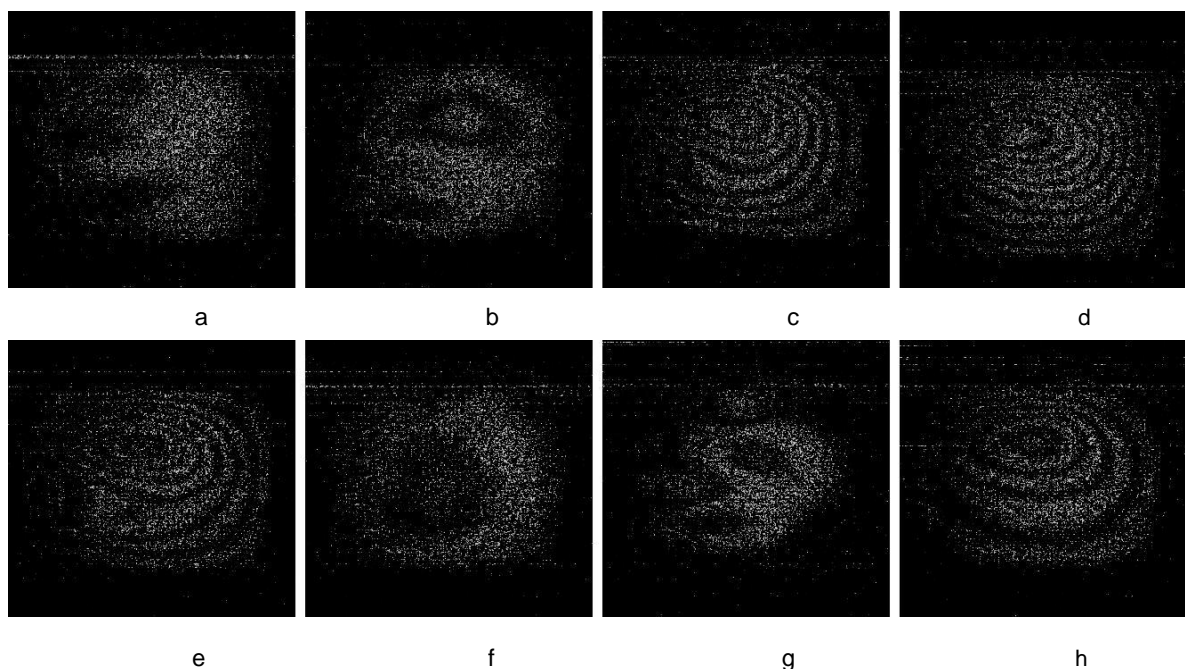


Fig. 5. Fringe patterns representing the membrane under vibration. The CMOS camera is configured at 5000 fps allowing the formation of hundreds of fringe patterns. Here there are only 8 of them selected to be processed by the proposed technique, which are the 5, 15, 25, 35, 45, 55, 65 and 75 respectively for a to h.

The recovered phase for each fringe pattern is shown in Fig. 6. From these images, it is possible to select a specific pixel to graphic its value of phase at different times in order to graph the behavior of the pixel along the time. This will give an overview of the time-dependent behavior of each selected point of the membrane. In the

same way, it is possible to select a specific profile of the membrane to register the spatial behavior of it. Fig. 7 shows the temporal evolution at a specific point selected in a particular  $(x, y)$  pixel.

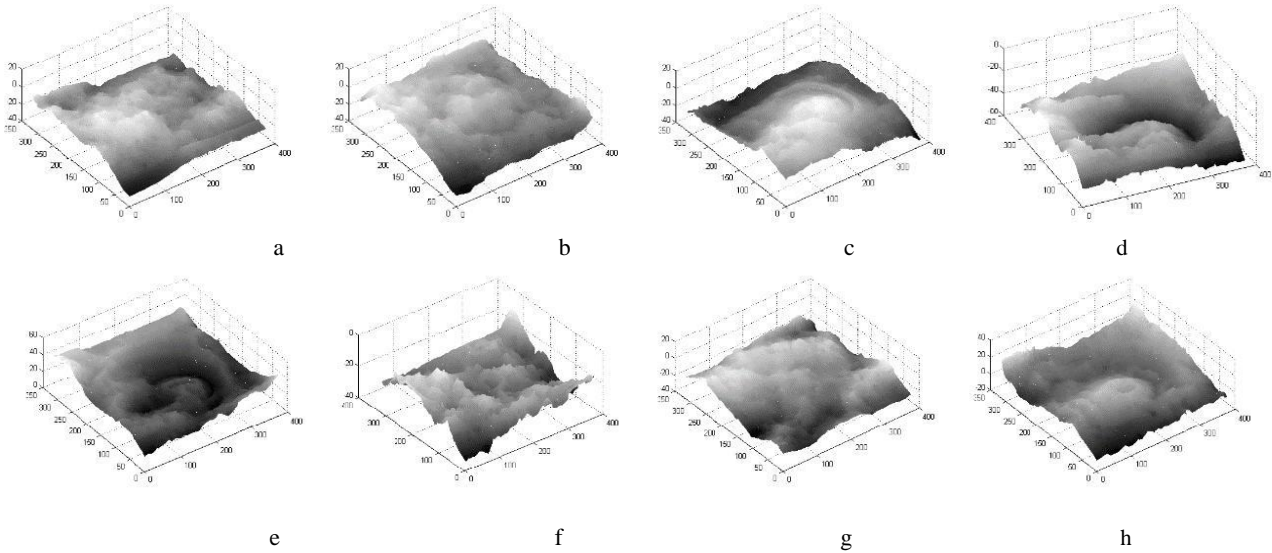


Fig. 6. Phase recovered from each fringe pattern shown in Fig. 5.

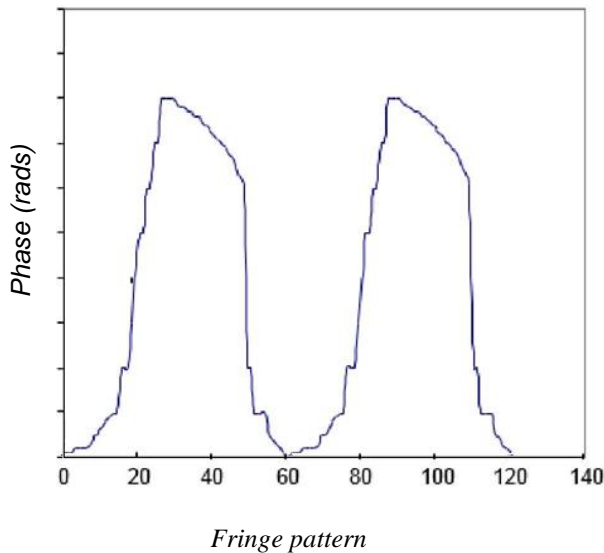


Fig. 7. Temporal phase evolution of a specific  $(x, y)$  pixel. 120 fringe patterns were enough to plot two full cycles of vibration, as it can be seen.

Only 120 fringe patterns were plotted in Fig. 7 covering 2 complete cycles of vibration. Each of the maximum value of phase per cycle are separated by 60 fringe patterns. Because of the CMOS camera was working at 5000 fps and only 60 fringe patterns are needed to cover a full vibration cycle, it is possible to calculate the

frequency of vibration of the membrane giving as a resulted frequency 81.96 Hz.

#### 4. Conclusions

In conclusion, a simple ESPI system using normal optical elements to obtain vibrational amplitude and phase measurements was implemented. The use of algorithms for phase recovery from a single fringe pattern reduces the number of optical elements on the ESPI setup increasing the possibility of applying this technique in non-destructive testing along industrial use.

The proposed technique for phase recovery of single fringe patterns applied to a HSESPI system is a great combination of techniques that could give excellent results of deformation measurements under difficult conditions. With the combination of these two techniques, it is not necessary any kind of synchronization, a carrier introduction or any extra component to get a measure.

In this paper, we have presented an idea of combination of techniques available to give an application at industrial level. It must be emphasized that every day there are new techniques, new proposals, new phase recovery algorithms, etc. This indicates that the ESPI technique will still maintain a great interest among researchers for a long time.

### Acknowledgement

The authors would like to acknowledge partial financial support from Consejo Nacional de Ciencia y Tecnología, Grant 157594.

### References

- [1] J. N. Butters, J. A. Leeudertz, Transactions of the institute of measurement and control, **4**(12), 349 (1971).
- [2] A. Macovski, S. D. Ramsey, L. F. Schaefer, Appl. Opt., **10**, 2722 (1971).
- [3] O. Schwomma, Austria patent 298 830 (1972).
- [4] R. J. Pryputniewicz, K. A. Stetson, Proc. SPIE, **1162**, 456 (1989).
- [5] A. R. Ganesan, R. S. Sirohi, (DSPI), Proc. SPIE. **954**, 327 (1988).
- [6] J. R. Tyrer, Proc. SPIE, **604**, 95 (1986).
- [7] R. Jones, C. Wykes, Optic Acta, **24**(5), 533 (1977).
- [8] K. Creath, Appl. Opt., **24**, pp. 3053 (1985).
- [9] Ángel F. Doval, Meas. Sci. Technol. **11**, R1 (2000).
- [10] Ole J. Løkberg, Physics in Technology, **11**, 16 (1980).
- [11] Ole J. Løkberg, Speckle Metrology, ed, R. S. Sirohi, Marcel Dekker, Inc. (1993).
- [12] M. Bahich, M. Afifi, E. Barj, Journal of computing, **2**(5), 1 (2010).
- [13] M. Servin, J. Marroquin, F. Cuevas, Appl. Opt., **36**, 4540 (1997).
- [14] M. Servin, J. Marroquin, J. A. Quiroga, J. Opt. Soc. Am. A, **21**, 411 (2004).
- [15] R. Legarda-S'aenz, M. Rivera, J. Opt. Soc. Am. A, **23**(11), 2724 (2006).
- [16] M. Rivera, J. Opt. Soc. Am. A, **22**, 1170 (2005).
- [17] J. C. Estrada, M. Servin, d J. L. Marroquin, Opt. Express, **15**, 2288 (2007).
- [18] Q. Kemao, H. Soon, Opt. Lett., **32**, 127 (2007).
- [19] J. A. Quiroga, D. Crespo, J. A. Gomez-Pedrero, Proc. of SPIE, **6616**, 66163Y-1-10, (2007).
- [20] K. G. Larkin, D. J. Bone, M. A. Oldfield, JOSA A **8**, 1862-70 (2001).
- [21] M. Servin, J. A. Quiroga, J. L. Marroquín, JOSA A **20**, 925-934 (2003).

---

\*Corresponding author: dgutierrez@cboaa.com